Coherent π° photo-production on ^{4}He at Intermediate Energies with Polarized Photons

V. Bellini [a,b], M. Capogni [c,d], A. Caracappa [e], L. Casano [c], A. D'Angelo [c], F. Ghio [f], B. Girolami [f], S. Hoblit [e], L. Hu [c], M. Khandaker [e,g], O. C. Kistner [e], L. Miceli [e], D. Moricciani [c], A. M. Sandorfi [e], C. Schaerf [c,d], M. L. Sperduto [a,b], C. E. Thorn [e]

[a] *Physics Department, University of Catania,Corso Italia 57, I-95129, Catania, Italy*

[b] *INFN-LNS, Via S. Sofia 44, I-95125, Catania, Italy*

[c] *INFN-Roma 2, Via della Ricerca Scientifica 1, I-00133, Rome, Italy*

[d] *Physics Department, University of Rome "Tor Vergata", Via della Ricerca Scientifica 1, I-00133, Rome, Italy*

[e] *Physics Department, Brookhaven National Laboratory, Upton N.Y. 11973, USA*

[f] *Istituto Superiore di Sanitá and INFN-ISS, Viale Regina Elena 299, I-00161, Rome, Italy*

[g] *Physics Department, Virginia Polytechnic Inst. & State University, Blacksburg, VA 24061, USA*

The reaction $^4\mathrm{He}(\vec{\gamma},\pi^\circ)^4\mathrm{He}$ has been studied with the LEGS tagged, polarized gamma ray beam. Data are presented at laboratory angles of $31^\circ, 45^\circ, 72.5^\circ, 90^\circ, 110^\circ$and $130^\circ$for incoming photon energies of 206, 219, 232, 245, 259, 274, 289, 306 and 322 MeV. The unpolarized cross sections are compared with the $\Delta - hole$ theoretical model results available in literature. The measured photon beam asymmetry is -1 as expected from conservation of angular momentum and parity.

PACS: 25.20 D, 24.70, 29.27 H

1 Introduction

Elastic Compton scattering and coherent π° photoproduction provide a complementary tool to pion scattering for the study of the interaction of pions with nucleons and nuclei. In contrast to pion scattering, the mean free path for photon interactions in nuclear matter is much larger than the nuclear size, which allows the photon to deeply penetrate the nuclear interior. Furthermore, the distortion of the photon field by the Coulomb field of the nucleus is negligible.

A photon with an energy around 300 MeV can excite the P_{33} Δ isobar inside the nucleus which can decay with the emission of a pion or a photon. The production, propagation and decay of the Δ isobar inside the nucleus is influenced by several factors: Fermi motion, Δ nucleus interactions and $\Delta - N$ binding, Pauli blocking of the Δ decay, final state interaction of the emitted pion, and the couplings among the different decay channels (photon emission, pion emission and various forms of nuclear disintegration). Several $\Delta - hole$ models have been developed to take these effects into account [1–4].

The angular dependence of the cross section for coherent π° photoproduction on ^{4}He, $\vec{\gamma} + {}^4\mathrm{He} \rightarrow \pi^\circ + {}^4\mathrm{He}$, with linearly polarized photons is largely determined by the fact that (a) the spin of the ^{4}He nucleus and the π° are both zero and (b) the π° is a pseudoscalar particle. With only three vectors available, the only way to form a pseudoscalar operator is $\vec{\varepsilon} \cdot \vec{k} \times \vec{q}$ [5], where in the center-of-mass frame (cm), $\vec{\varepsilon}$ is the polarization vector of the photon, $\vec{k}$ is the momentum of the photon, and $\vec{q}$ is the momentum of the pion.

Therefore, when the polarization vector, $\vec{\varepsilon}$, is parallel to the reaction plane (the plane of the photon and the pion) the transition matrix element is zero, so that

$$\frac{d\sigma_{\|}}{d\Omega} = 0, \tag{1}$$

and the asymmetry for linearly polarized photons is -1,

$$\Sigma = \frac{\frac{d\sigma_{\|}}{d\Omega} - \frac{d\sigma_{\perp}}{d\Omega}}{\frac{d\sigma_{\|}}{d\Omega} + \frac{d\sigma_{\perp}}{d\Omega}} = -1 \tag{2}$$

where

$$\frac{d\sigma_{\perp}}{d\Omega} \neq 0 \tag{3}$$

is the differential cross section with the photon polarization perpendicular to the reaction plane.

In conclusion, the experimental cross section is expected to take the form,

$$\frac{d\sigma}{d\Omega}(E_\gamma, \vartheta_{\pi^\circ}^{CM}, \varphi_{\pi^\circ}) = \frac{d\sigma}{d\Omega}_{unp.}(E_\gamma, \vartheta_{\pi^\circ}^{CM})\big(1 - P\cos 2\varphi_{\pi^\circ}\big) \tag{4}$$

where P is the polarization of the photon beam.

This result makes the study of the azimuthal angular distribution in this reaction an attractive way to measure the polarization of gamma-ray beams. On the other hand, the unpolarized cross section contains all the information on the reaction mechanism we can learn from this process, since the photon is the only particle which can be polarized.

2 Experimental Set-up

The experimental data have been collected with the LEGS [6,7] polarized and tagged gamma-ray beam produced by the backward Compton scattering of laser light against the high energy electrons circulating in the storage ring of the National Synchrotron Light Source (NSLS) at Brookhaven National Laboratory. With an electron energy of 2.6 GeV and using the Green and UV lines of an Argon Ion laser, we have produced two different photon spectra with maximum energies of 225 MeV and 317 MeV. The polarization of the gamma-ray depends on the ratio between its energy and the maximum energy produced, $E_\gamma/E_{\gamma max}$. Therefore repeating a measurement at the same E_γ with different $E_{\gamma max}$ provides a comparison of the results obtained with two different gamma-ray polarizations.

The beam had an intensity of the order of 4×10^6 γ/s and the tagging hodoscope provided an energy resolution of about 5 MeV (FWHM) [7].

The target consisted of a Nickel cylinder, closed on both sides by two hemispheres, with a total length $l = 10$ cm and a diameter of 5 cm. It was filled with liquid ^{4}He at a temperature of 3.9°K and a pressure slightly above one atmosphere. The temperature and pressure of the target where continuously monitored during the experiment, and the resulting ^{4}He density was $\varrho = 0.140 \pm 0.001$ g/cm^3.

The higher energy of the two photons from the π° decay was detected by a high resolution, cylindrical NaI(Tl) scintillator 48 cm diameter by 48 cm deep (referred from now on as the 48cm NaI). It was surrounded by an anti-coincidence shield (the Annulus) to veto cosmic rays and reject events where appreaciable energy was lost by the electromagnetic showers in the 48cm NaI. The acceptance solid angle was defined by a Lead collimator and an antico-incidence plastic scintillator (the Paddle) placed between the collimator and the NaI detector. The accepted solid angle of the detector was $\Delta\Omega = 0.13$ sr. The whole system was encapsulated in a 5cm thick lead annulus.

The lower energy photon from the π° decay was detected by eight NaI(Tl) bars (the Bars) $10 \times 10 \times 35$ cm^3 placed around the detector with their axis parallel to the beam line as indicated in fig. 1. Their average efficiency for the detection of the lower energy photon was 68%, when the higher energy photon triggered the 48cm NaI detector.

A pulse in the 48cm NaI corresponding to an energy deposition larger than 120 MeV, in coincidence with an event in the tagging hodoscope triggered the acquisition system. A recorded event contained the amplitudes (ADC) and the time of flights (TOF) of the pulses in the 48cm NaI, the Annulus, the Paddle, the Bars and the TOF of all tagging counters.

Data were collected with the laser light polarized in the horizontal and the

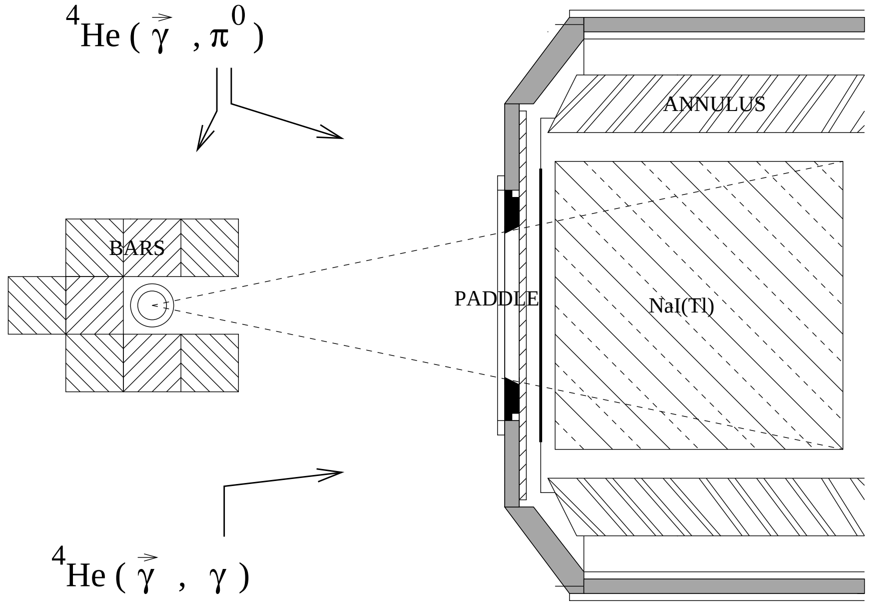

Fig. 1. Sketch of the experimental set-up

vertical planes, changing the direction of polarization at random intervals of time between 150 and 450 seconds. This provides gamma-rays polarized in the reaction plane and perpendicularly to it, respectively.

3 Data Analysis

Data were taken simultaneously for coherent π° photoproduction and Compton scattering on ^{4}He. Elastically scattered photons provided a continuous monitoring of the energy calibration of the 48cm NaI detector. The photopion production cross section was a factor of about fifty larger than that for elastic scattering. This is clearly indicated in fig. 2 where we have plotted the amplitude of the 48cm NaI pulses versus the tagging channel for a given angular position of the counter.

Four reactions contribute in fig. 2:

$$\vec{\gamma} + {}^4\mathrm{He} \rightarrow \gamma' + {}^4\mathrm{He}, \tag{5}$$

$$\vec{\gamma} + {}^4\mathrm{He} \rightarrow \pi^\circ + {}^4\mathrm{He}, \tag{6}$$

$$\vec{\gamma} + {}^4\mathrm{He} \rightarrow \pi^\circ + X, \tag{7}$$

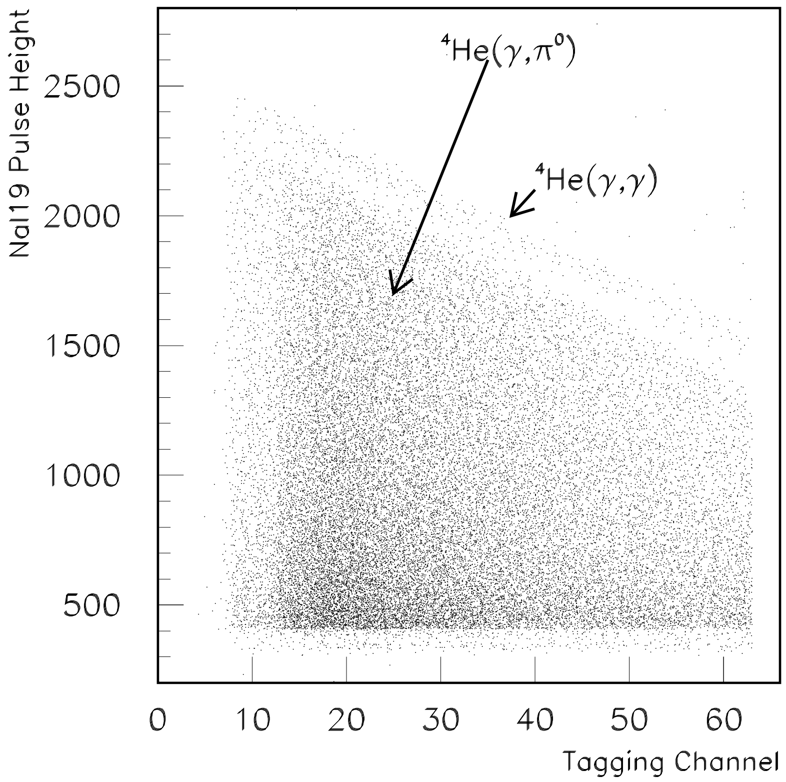

Fig. 2. Bidimensional plot of NaI Pulse Amplitude versus Tagging Channel

$$\vec{\gamma} + {}^4\mathrm{He} \rightarrow \gamma' + X, \tag{8}$$

where X indicates any four nucleon state (predominantly: T + p and ^{3}He + n).

Reaction 5 is clearly separated in all plots. The cross section for reaction 8 is much smaller than that of 6 or 7 and its contribution can be neglected. The threshold for reaction 7 is about 21 MeV higher than that for reaction 6. Therefore there is a kinematic region where reaction 6 can be isolated. The procedure followed to calculate its contribution is indicated in fig. 3 [8]. For each tagging channel, we have simulated (using a GEANT 3.21 code) the gamma-ray spectra in our detector produced by the π° decay coming from reactions 6 and 7. For reaction 7 we have assumed a phase space distribution for the three-body final state π° p T (or π° n ^{3}He). A linear combination of the coherent and incoherent spectra has been compared with the experimental data and the best-fit value of its coefficients determined.

In fig. 3 we show the result at a laboratory angle $\theta = 90^\circ$ for the 48cm NaI and an energy bin centered at 274 MeV for the incoming gamma-ray. The solid line indicates the experimental data (EXP.DATA), and the broken line the simulated predictions (SIM.DATA). The latter is the sum of the two components shown as the dotted line, from reaction 6, and the dot-dash line, from reaction 7. Events on the right hand side of the vertical arrow have been used to calculate a cross section for reaction 6. The simulation has also provided the efficiency of our detector, as a function of the position of the

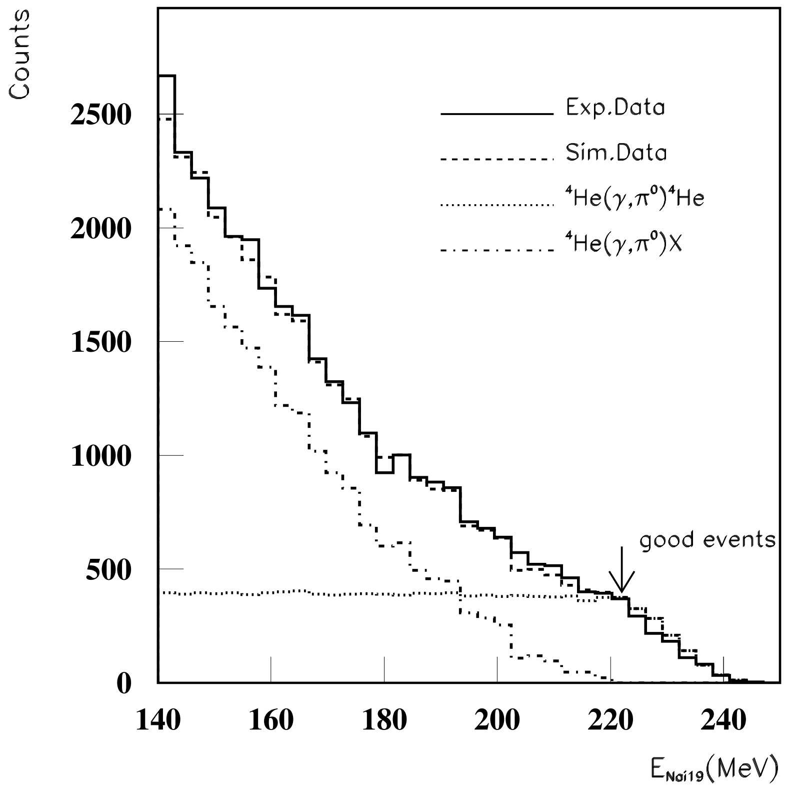

Fig. 3. Comparison between experimental and simulated NaI spectra

arrow, the energy deposited in the Annulus, and the efficiency of the Bars. The values of the bar efficiency predicted by Monte-Carlo have been confirmed by the experimental data.

The data have been corrected for accidental coincidences (between the 48cm NaI and the tagger), empty target background and cosmic rays. At the backward angles the cross section is smaller and the cosmic ray background is non-negligible. These cosmic rays were effectively rejected by requiring no more than 30 MeV be deposited in the plastic annulus. Any remaining cosmic contamination has been removed through the subtraction of accidental coincidences with the tagger.

When a π° decays, the gamma-ray emitted in a direction very close to that of the π° carries the maximum energy. Since our procedure for isolating coherent π° production relies on selecting only the maximum energy photons, the mean angle of the 48cm NaI is effectively the mean π° angle.

4 Experimental results

A simulation of the gamma-ray beam production dynamics, which took into account its collimation as well as the divergence of the primary electron beam, was used to derive the theoretical values of the gamma-ray beam spectrum and polarization as a function of E_γ. These values were used to calculate the experimental values of the unpolarized cross section and beam asymmetry according to the formula:

$$\frac{d\sigma}{d\Omega}(E_\gamma, \vartheta^{CM}_{\pi^\circ}, \varphi_{\pi^\circ}) = \frac{d\sigma}{d\Omega}_{unp.}(E_\gamma, \vartheta^{CM}_{\pi^\circ})\left[1 + P\Sigma(E_\gamma, \vartheta^{CM}_{\pi^\circ}) \cos 2\varphi_{\pi^\circ}\right] \quad (9)$$

where $\varphi_{\pi^\circ} = 0$ and $\varphi_{\pi^\circ} = \pi/2$ for the laser light polarized in the horizontal and vertical plane respectively. (Comparison of the results with equation 4 provides an explicit test of the expected asymmetry.)

Using two different laser lines, in the green and the UV , the two energy bins at 219 and 232 MeV could be measured twice with two different gamma-ray spectra and polarizations. This provided an experimental confirmation of the calculations of the gamma-ray beam properties. The data were collected at six values of the pion angle:

$$\theta^{CM}_{\pi^\circ} = 33^\circ, 47^\circ,\ 75^\circ,\ 93^\circ,\ 113^\circ,\ 133^\circ \quad (10)$$

and divided into nine energy bins centered at the gamma ray energies:

$$E_\gamma = 206,\ 219,\ 232,\ 245,\ 259,\ 274,\ 289,\ 306,\ 322 \text{ MeV}. \quad (11)$$

The values of the unpolarized cross section are reported in Table 1 and indicated in figures 4 and 5. The sources of possible systematic scale uncertainties are summarized in table 2. Adding these in quadrature gives a total of 3.1%.

In the figures the data are compared with those of previous experiments and theoretical calculations where available. To this end the data at $E_\gamma = 289$ MeV are represented as a function of the angle in the laboratory. The data at $E_\gamma = 322$ MeV are compared with calculations at 330 MeV from [3]. The same data are also shown as a function of the beam energy for different pion angles in fig. 6.

The values obtained for the beam asymmetry are indicated in fig. 7. All 54 measurements are compatible with -1, as expected, with a χ^2 equal to 1.39.

5 Conclusions

Our results for the unpolarized cross sections, collected simultaneously in a wide energy range and for a large angular range, provide a useful test of the $\Delta - hole$ model theory.

There is a good agreement between previous experimental data and ours. The $\Delta - hole$ model reproduces very well the experimental data for the incoming photon energy $E_\gamma = 290$ MeV.

At higher energy the $\Delta - hole$ model reproduces the cross section in the backward direction but overestimates the experimental results at forward angles. At lower gamma ray energies these new results bring useful information to the physical models in a region dominated by the non-resonant contributions.

Finally, the photon beam asymmetry agrees with the expected value for all the measured energies and angles. This confirms the high degree of polariza-

ϑ^{LAB} (deg) / E_γ^{LAB} (MeV)	$31°$	$45°$	$72.5°$	$90°$	$110°$	$130°$
206	10.28 ± 0.47	15.62 ± 0.79	16.21 ± 0.59	13.94 ± 0.36	11.89 ± 0.42	4.53 ± 0.17
	$32.5°$	$46.6°$	$74.8°$	$93.1°$	$113°$	$133°$
219	13.04 ± 0.55	22.20 ± 0.86	27.45 ± 0.60	21.15 ± 0.38	14.39 ± 0.33	5.23 ± 0.16
	$32.5°$	$46.7°$	$74.9°$	$93.2°$	$113°$	$133°$
232	22.24 ± 0.70	25.74 ± 0.88	31.29 ± 0.80	23.66 ± 0.44	12.49 ± 0.31	5.20 ± 0.17
	$32.8°$	$46.8°$	$75.1°$	$93.4°$	$113°$	$133°$
245	29.37 ± 1.40	39.53 ± 2.08	31.32 ± 0.85	23.58 ± 0.52	8.16 ± 0.29	3.51 ± 0.23
	$33.0°$	$47.0°$	$75.3°$	$93.6°$	$114°$	$133°$
259	31.07 ± 1.39	41.27 ± 2.22	34.56 ± 0.90	21.20 ± 0.52	7.38 ± 0.30	2.25 ± 0.17
	$32.9°$	$47.0°$	$75.3°$	$93.4°$	$114°$	$133°$
274	38.04 ± 1.49	60.38 ± 2.61	40.83 ± 1.03	19.42 ± 0.49	1.23 ± 0.22	0.97 ± 0.16
	$32.9°$	$47.1°$	$75.4°$	$93.5°$	$113°$	$133°$
289	47.45 ± 1.65	56.87 ± 2.08	36.20 ± 0.95	12.33 ± 0.35	4.87 ± 0.26	1.18 ± 0.15
	$33.0°$	$47.3°$	$75.6°$	$93.7°$	$114°$	$133°$
306	45.91 ± 1.56	54.24 ± 2.49	26.57 ± 0.82	8.16 ± 0.41	3.19 ± 0.19	0.65 ± 0.07
	$33.2°$	$47.5°$	$76.0°$	$93.1°$	$113°$	$133°$
322	35.94 ± 2.42	31.94 ± 2.86	15.38 ± 1.05	5.39 ± 0.48	1.19 ± 0.29	0.68 ± 0.11
	$32.9°$	$47.4°$	$76.0°$	$93.8°$	$114°$	$133°$

Table 1
Experimental cross sections (μb/sr) for ^{4}He and π° CM angles.

Uncertainty		Source
Solid angle :	2.5%	position of NaI detector
Analysis effeciency :	1.0%	effect of resolution on “arrow cut”
Target density :	0.7%	variations in T and P
Target length :	0.2%	target
Flux normalization :	1.0%	time variations
Flux normalization :	1.0%	rate variations
Total :	3.1%	quadrature sum

Table 2
Systematic scale uncertainties on the ^{4}He(γ,π°) cross section.

tion of the photon beams obtained by the technique of backward Compton scattering [12]. Very recently this technique has been used to measure the linear polarization of a gamma ray beam produced by coherent bremsstrahlung [13]. This latter process is much more complex than the simple Klein-Nishina scattering of light from free electrons in vacuum, and there the $^4\mathrm{He}(\vec{\gamma},\pi^\circ)$ asymmetry has provided an essential polarimeter.

This work was supported by the Istituto Nazionale di Fisica Nucleare, Italy, the U.S. Department of Energy under contract No. DE-AC02-76CH00016, and the National Science Foundation. We are indebted to Mr. Frank Lincoln and Mr. Anthony Kuczewski for their assistance during the measurements.

References

[1] W. Weise *Nuclear Physics* **A358** (1981) 163

[2] E. Oset and W. Weise *Nuclear Physics* **A368** (1981) 375-393

[3] J.H. Koch and E.J. Moniz *Phys Rev.* **C27** (1983) 751

[4] J. H. Koch, E.J. Moniz and N. Ohtsuka *Annals of Physics* **154** (1984) 99-160

[5] N. Cabibbo *Phys. Rev. Lett.* **7** (1961) 386

[6] A.M. Sandorfi et al. *IEEE Trans.* **NS-30** (1983) B 3093

[7] C.E.Thorn et al. *Nucl. Instr. Meth.* **A285** (1989) 447

[8] M. Capogni Ph. D. Thesis, Univ. of Rome "Tor Vergata" (1998) unpublished

[9] D.R. Tieger et al. *Phys. Rev. Lett.* **53** (1984) 755

[10] J. LeFrancois et al. *Nuovo Cimento* **65A** (1970) 333

[11] J.W. Staples Ph. D. Thesis, Univ. of Illinois (1969) unpublished

[12] D. Babusci et al. *La Rivista del Nuovo Cimento* **19** (1996) 5

[13] A. Kraus et al. *Phys. Rev. Lett.* **79** (1997) 3834

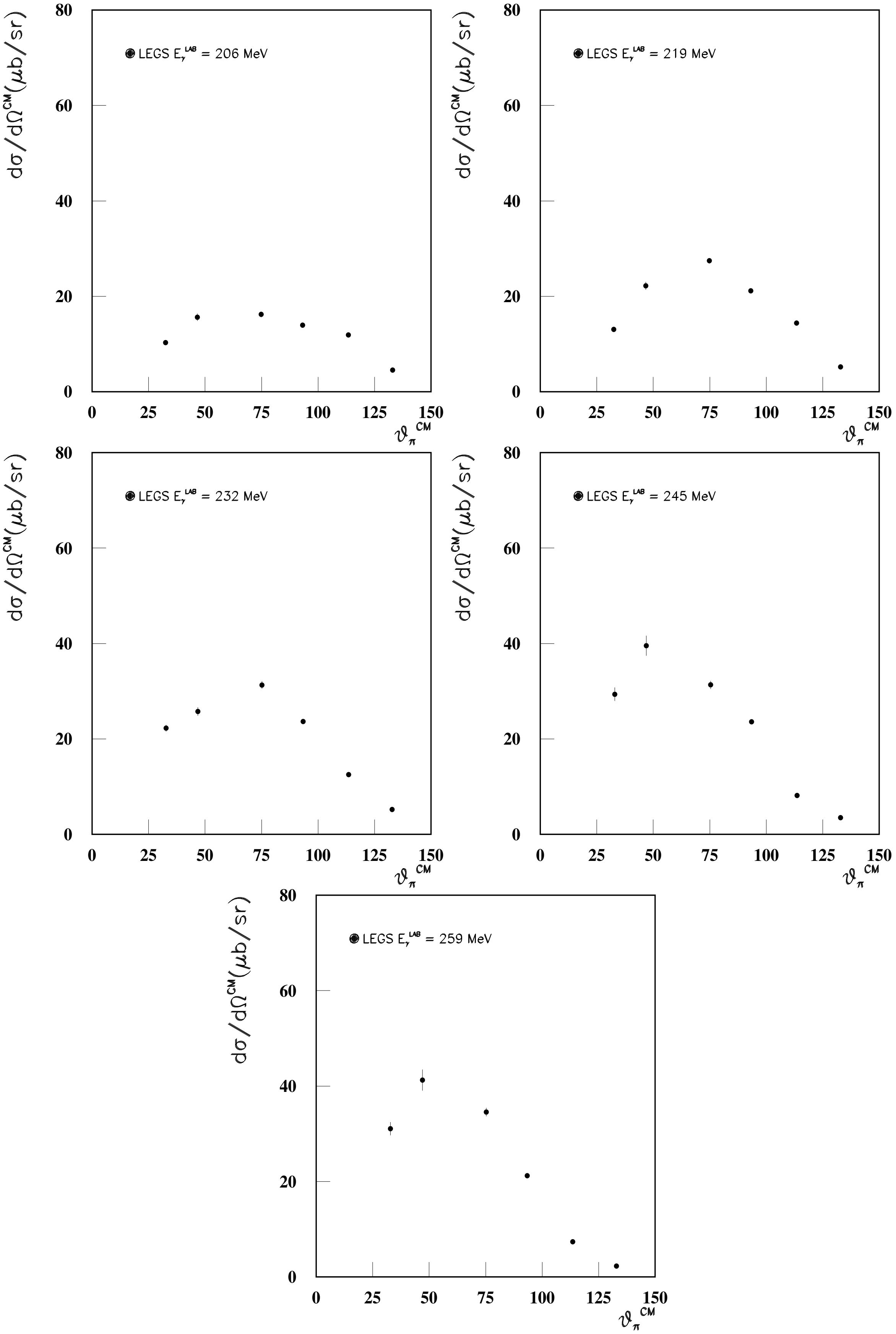

Fig. 4. Unpolarized cross Section ranging from 206 to 259 MeV.

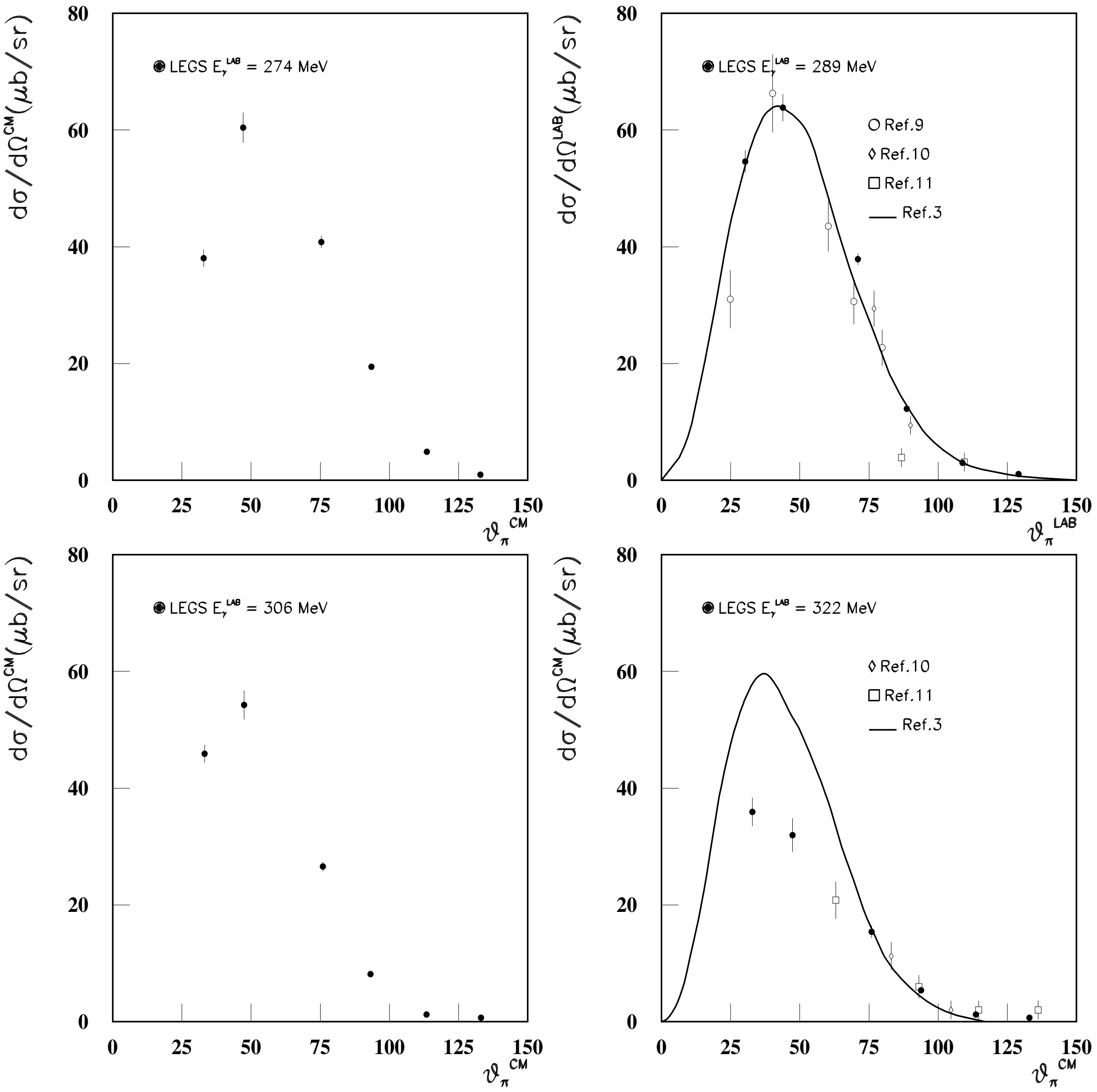

Fig. 5. Unpolarized cross Section ranging from 274 to 322 MeV. (Note that all are plotted against c.m. angle, except 289 MeV which is plotted against lab angle for the purpose of comparing directly with published data.)

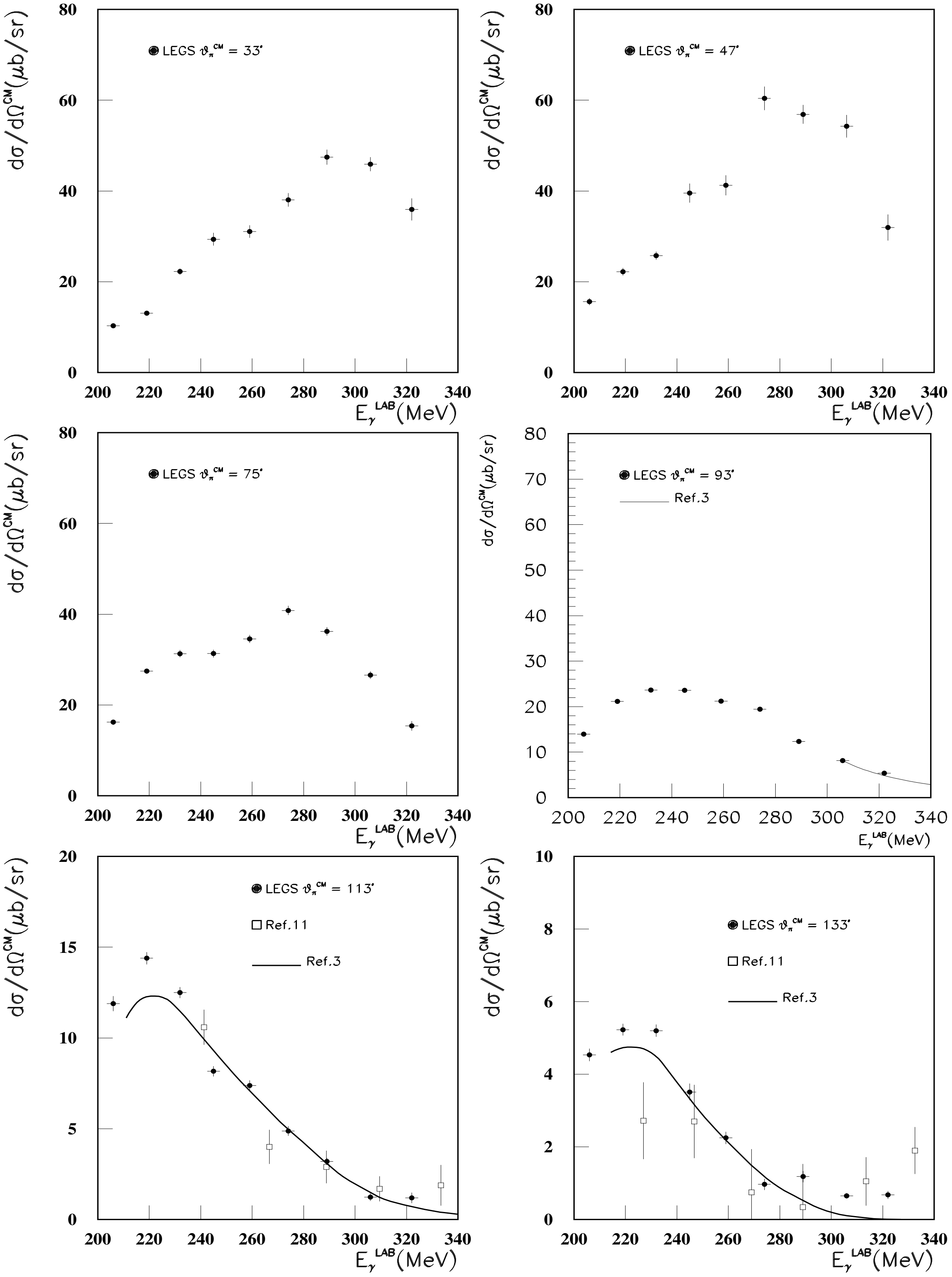

Fig. 6. Unpolarized cross Section for the different ϑ_{π° as function of the energy of incoming photon beam

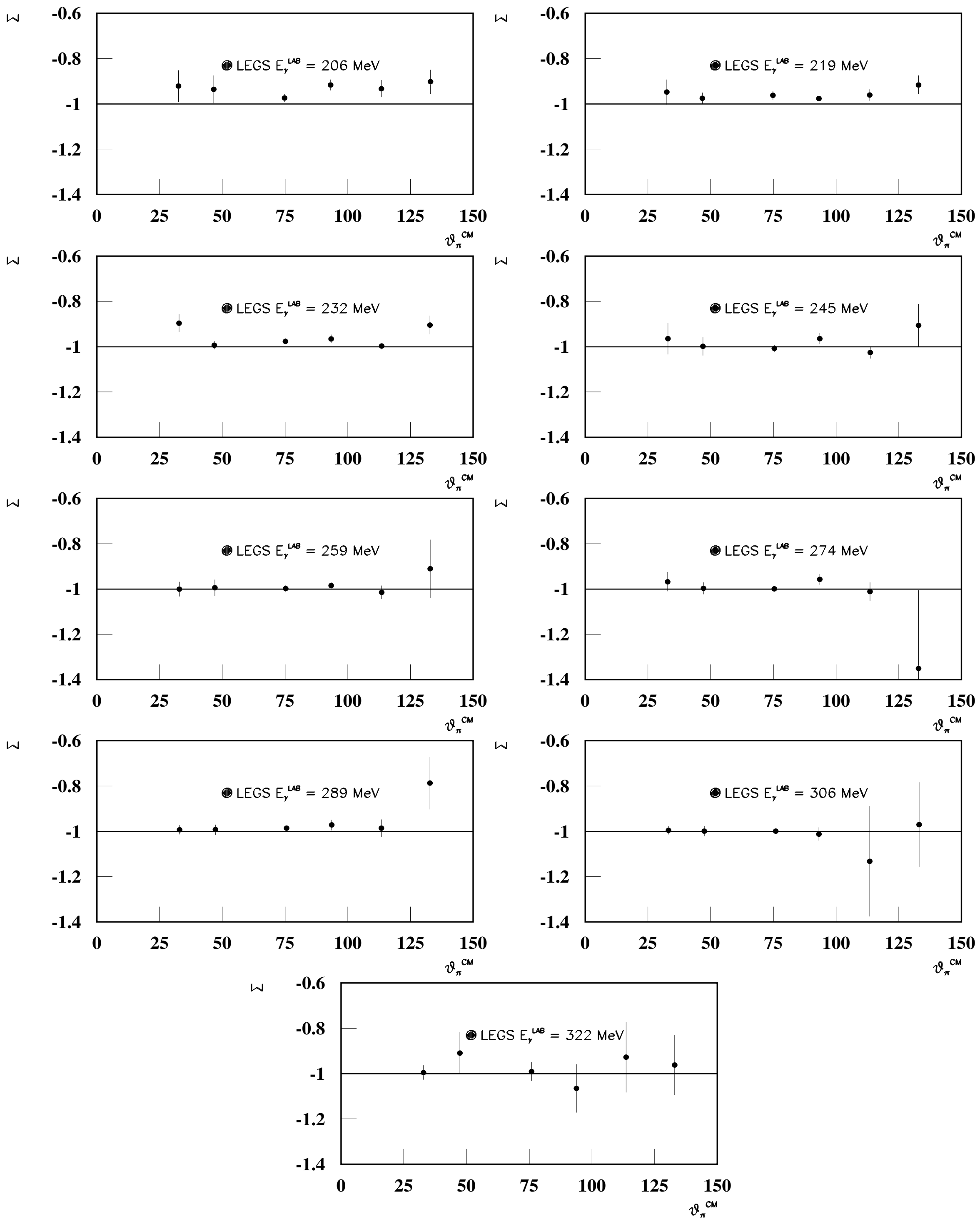

Fig. 7. Photon beam asymmetry for all the energy bins.